

Active and Passive Fields in Turbulent Transport: the Role of Statistically Preserved Structures

Emily S.C. Ching,¹ Yoram Cohen,² Thomas Gilbert,² and Itamar Procaccia²

¹*Department of Physics, The Chinese University of Hong Kong, Sha Tin, Hong Kong*

²*Dept. of Chemical Physics, The Weizmann Institute of Science, Rehovot 76100, Israel*

(Dated: November 5, 2018)

We have recently proposed that the statistics of *active* fields (which affect the velocity field itself) in well-developed turbulence are also dominated by the Statistically Preserved Structures of auxiliary *passive* fields which are advected by the same velocity field. The Statistically Preserved Structures are eigenmodes of eigenvalue 1 of an appropriate propagator of the decaying (unforced) passive field, or equivalently, the zero modes of a related operator. In this paper we investigate further this surprising finding via two examples, one akin to turbulent convection in which the temperature is the active scalar, and the other akin to magneto-hydrodynamics in which the magnetic field is the active vector. In the first example, all the even correlation functions of the active and passive fields exhibit identical scaling behavior. The second example appears at first sight to be a counter-example: the statistical objects of the active and passive fields have entirely different scaling exponents. We demonstrate nevertheless that the Statistically Preserved Structures of the passive vector dominate again the statistics of the active field, except that due to a dynamical conservation law the amplitude of the leading zero mode cancels exactly. The active vector is then dominated by the sub-leading zero mode of the passive vector. Our work thus suggests that the statistical properties of active fields in turbulence can be understood with the same generality as those of passive fields.

PACS numbers: 47.27.-i

I. INTRODUCTION

The aim of this paper is to address the statistical physics of so called “active” fields in developed fluid turbulence. These are fields that differ from the fundamental fluid velocity field $\mathbf{u}(\mathbf{r}, t)$, but that interact with the velocity field in an essential way, for example effecting a significant change in the scaling exponents of the velocity correlation functions from the classical Kolmogorov exponents. For the sake of concreteness we will focus on two generic examples with very different interactions between the active and the velocity fields.

The first is thermal turbulent convection, in which the temperature field $T(\mathbf{r}, t)$ is driving the velocity field through buoyancy effects. In the Boussinesq approximation the temperature equation reads like a standard forced scalar advection problem,

$$\frac{\partial T(\mathbf{r}, t)}{\partial t} + \mathbf{u}(\mathbf{r}, t) \cdot \nabla T(\mathbf{r}, t) = \kappa \nabla^2 T(\mathbf{r}, t) + f(\mathbf{r}, t). \quad (1)$$

Here κ is the thermal diffusivity and $f(\mathbf{r}, t)$ is a white random force of zero mean with compact support in \mathbf{k} -space, acting on the largest scales of the order of the outer scale L only. The velocity field is affected by the temperature. For an incompressible fluid of unit density [1] (dropping the dependence on (\mathbf{r}, t) for brevity),

$$\frac{\partial \mathbf{u}}{\partial t} + \mathbf{u} \cdot \nabla \mathbf{u} = -\nabla p + \nu \nabla^2 \mathbf{u} + \alpha g T \hat{z}. \quad (2)$$

Here p , ν , α , g and \hat{z} are the pressure, kinematic viscosity, volume expansion coefficient, acceleration due to gravity and a unit vector in the upward direction respectively. The appearance of T in the equation for \mathbf{u} is crucial, and

changes the scaling exponents of \mathbf{u} . When the conditions are right it may even change the scaling exponents from Kolmogorov to Bolgiano (up to anomalies) [1].

The second example is that of magneto-hydrodynamics (MHD), in which the magnetic field $\mathbf{b}(\mathbf{r}, t)$ is driving the velocity field $\mathbf{u}(\mathbf{r}, t)$ according to [2]

$$\begin{aligned} \frac{\partial \mathbf{u}}{\partial t} + \mathbf{u} \cdot \nabla \mathbf{u} &= -\nabla p + \mathbf{b} \cdot \nabla \mathbf{b} + \nu \nabla^2 \mathbf{u}, \\ \frac{\partial \mathbf{b}}{\partial t} + \mathbf{u} \cdot \nabla \mathbf{b} &= \mathbf{b} \cdot \nabla \mathbf{u} + \kappa \nabla^2 \mathbf{b} + \mathbf{f}. \end{aligned} \quad (3)$$

These equations of motion conserve (in the inviscid, unforced limit) three quadratic invariants, i. e. the energy, magnetic helicity and cross helicity [3]

Our main interest is in the properties of the statistical objects characterizing the active fields, including their anomalous scaling. Here “anomalous scaling” means that multi-point correlation functions are homogeneous functions of their arguments, with exponents that cannot be guessed from dimensional analysis. Thus for example the field $\phi(\mathbf{r}, t)$ (with ϕ being T or \mathbf{b} respectively) has simultaneous multi-point correlation functions

$$F^{(m)}(\mathbf{r}_1, \mathbf{r}_2, \dots, \mathbf{r}_m) \equiv \langle \phi(\mathbf{r}_1, t) \phi(\mathbf{r}_2, t) \dots \phi(\mathbf{r}_m, t) \rangle_f, \quad (4)$$

where pointed brackets with subscript f refer to averaging over the statistics of the advecting velocity field and of the forcing. The forcing is taken to be white random noise with zero mean. When the forcing is stationary in time this object is *time independent*. Anomalous scaling means that

$$F^{(m)}(\lambda \mathbf{r}_1, \dots, \lambda \mathbf{r}_m) = \lambda^{\zeta_m} F^{(m)}(\mathbf{r}_1, \dots, \mathbf{r}_m), \quad (5)$$

with ζ_m having a non-trivial dependence on m . In what follows we will assume that the advecting velocity field itself is fully turbulent, and that its correlation functions are also exhibiting scaling behavior like Eq. (5).

The main point of this paper is that the statistical theory of the active fields calls for consideration of auxiliary passive fields that satisfy the same equations of motion as the active fields, but *do not* affect the velocity field itself. In other words, For the two problems at hand we consider the following equations of motion :

$$\begin{aligned} \frac{\partial \mathbf{u}}{\partial t} + \mathbf{u} \cdot \nabla \mathbf{u} &= -\nabla p + \nu \nabla^2 \mathbf{u} + \alpha g T \hat{z} , \\ \frac{\partial T}{\partial t} + \mathbf{u} \cdot \nabla T &= \kappa \nabla^2 T + f , \\ \frac{\partial C}{\partial t} + \mathbf{u} \cdot \nabla C &= \kappa \nabla^2 C + \tilde{f} , \end{aligned} \quad (6)$$

on the one hand, and

$$\begin{aligned} \frac{\partial \mathbf{u}}{\partial t} + \mathbf{u} \cdot \nabla \mathbf{u} &= -\nabla p + \mathbf{b} \cdot \nabla \mathbf{b} + \nu \nabla^2 \mathbf{u} , \\ \frac{\partial \mathbf{b}}{\partial t} + \mathbf{u} \cdot \nabla \mathbf{b} &= \mathbf{b} \cdot \nabla \mathbf{u} + \kappa \nabla^2 \mathbf{b} + \mathbf{f} , \\ \frac{\partial \mathbf{q}}{\partial t} + \mathbf{u} \cdot \nabla \mathbf{q} &= \mathbf{q} \cdot \nabla \mathbf{u} + \kappa \nabla^2 \mathbf{q} + \tilde{\mathbf{f}} , \end{aligned} \quad (7)$$

on the other.

Note that the velocity field that appears in the equations for the passive fields is *the same* as the velocity field that results from solving the coupled equations of the associated equations for the active fields. The forcing terms \tilde{f} in Eq. (6) (resp. $\tilde{\mathbf{f}}$ in Eq. (7)) have the same statistics as the forcing terms f in Eq. (1) (resp. \mathbf{f} in Eq. (3)), but they must have different realizations. While it is not true of course that the statistics of the passive fields are independent of the statistics of the velocity fields, it is true that the statistics of the velocity fields are independent of the statistics of the passive forcing terms. This is, however, not the case with the active forcing terms since these forcing terms affect the active fields that affect in their turn the velocity fields. It is thus not at all evident at first sight that there should be any relation, a priori, between the statistics of the active fields and their passive counterparts. On the other hand, if there were such a relationship, this would be very advantageous, since the statistics of the passive fields is understood as explained next.

To understand the progress made in the context of passive fields [4, 5], note that the passive fields satisfy a linear equation of motion that can be written as

$$\frac{\partial \phi(\mathbf{r}, t)}{\partial t} = \mathcal{L} \phi(\mathbf{r}, t) + f(\mathbf{r}, t) , \quad (8)$$

with the actual form of the operator \mathcal{L} determined by the problem at hand. In recent work [6, 7] it was clarified why and how passive fields exhibit anomalous scaling, when the velocity field is a generic turbulent field. The key is to consider a problem associated with Eq. (8) which is

the *decaying problem* in which the forcing $f(\mathbf{r}, t)$ is put to zero. The problem becomes then a linear initial value problem,

$$\partial \phi / \partial t = \mathcal{L} \phi , \quad (9)$$

with a formal solution

$$\phi(\mathbf{r}, t) = \int d\mathbf{r}' \mathbf{R}(\mathbf{r}, \mathbf{r}', t) \phi(\mathbf{r}', 0) , \quad (10)$$

with the operator

$$\mathbf{R} \equiv T^+ \exp \left[\int_0^t ds \mathcal{L}(s) \right] , \quad (11)$$

and T^+ being the time ordering operator. Define next the *time dependent* correlation functions of the decaying problem:

$$G^{(m)}(\mathbf{r}_1, \dots, \mathbf{r}_m, t) \equiv \langle \phi(\mathbf{r}_1, t) \cdots \phi(\mathbf{r}_m, t) \rangle . \quad (12)$$

Here pointed brackets without subscript f refer to the decaying object in which averaging is taken with respect to realizations of the velocity field only. As a result of Eq. (10) the decaying correlation functions are developed by a propagator $\mathcal{P}_{\underline{\mathbf{r}}|\underline{\boldsymbol{\rho}}}^{(m)}$, (with $\underline{\mathbf{r}} \equiv \mathbf{r}_1, \mathbf{r}_2, \dots, \mathbf{r}_m$) :

$$G^{(m)}(\mathbf{r}_1, \dots, \mathbf{r}_m, t) = \int d\underline{\boldsymbol{\rho}} \mathcal{P}_{\underline{\mathbf{r}}|\underline{\boldsymbol{\rho}}}^{(m)}(t) G^{(m)}(\boldsymbol{\rho}_1, \dots, \boldsymbol{\rho}_m, 0) . \quad (13)$$

In writing this equation we made explicit use of the fact that the *initial* distribution of the passive field $\phi(\mathbf{r}, 0)$ is statistically independent of the advecting velocity field. Thus the operator $\mathcal{P}_{\underline{\mathbf{r}}|\underline{\boldsymbol{\rho}}}^{(m)}$ can be written explicitly

$$\mathcal{P}_{\underline{\mathbf{r}}|\underline{\boldsymbol{\rho}}}^{(m)}(t) \equiv \langle \mathbf{R}(\mathbf{r}_1, \boldsymbol{\rho}_1, t) \mathbf{R}(\mathbf{r}_2, \boldsymbol{\rho}_2, t) \cdots \mathbf{R}(\mathbf{r}_m, \boldsymbol{\rho}_m, t) \rangle . \quad (14)$$

The key finding [6, 7] is that the operator $\mathcal{P}_{\underline{\mathbf{r}}|\underline{\boldsymbol{\rho}}}^{(m)}$ possesses *left* eigenfunctions of eigenvalue 1, i. e. there exist time-independent functions $Z^{(m)}(\mathbf{r}_1, \mathbf{r}_2, \dots, \mathbf{r}_m)$ satisfying

$$Z^{(m)}(\mathbf{r}_1, \dots, \mathbf{r}_m) = \int d\underline{\boldsymbol{\rho}} \mathcal{P}_{\underline{\boldsymbol{\rho}}|\underline{\mathbf{r}}}^{(m)}(t) Z^{(m)}(\boldsymbol{\rho}_1, \dots, \boldsymbol{\rho}_m) . \quad (15)$$

The functions $Z^{(m)}$ are referred to as ‘‘Statistically Preserved Structures’’, being invariant to the dynamics, even though *the operator is strongly time dependent and decaying*. How to form, from these functions, infinitely many conserved variables in the decaying problem was shown in [6], and is discussed again in Sect. II B. The functions $Z^{(m)}(\underline{\mathbf{r}})$ are homogeneous functions of their arguments, with anomalous scaling exponents ζ_m :

$$Z^{(m)}(\lambda \underline{\mathbf{r}}) = \lambda^{\zeta_m} Z^{(m)}(\underline{\mathbf{r}}) + \dots \quad (16)$$

where ‘‘...’’ stand for subleading scaling terms. Since Eq. (15) contains $Z^{(m)}(\underline{\mathbf{r}})$ on both sides, the scaling exponent ζ_m cannot be determined from dimensional considerations, and it can be anomalous. More importantly,

it was shown that the correlation functions of the forced case, $F^{(m)}(\mathbf{r})$ Eq. (4), have exactly the same scaling exponents as $Z^{(m)}(\mathbf{r})$ [7]. In the scaling sense

$$F^{(m)}(\mathbf{r}) \sim Z^{(m)}(\mathbf{r}) . \quad (17)$$

This is how anomalous scaling in passive fields is understood. Lastly, we note that for the operator governing the time derivative of Eq. (12), $Z^{(m)}(\mathbf{r})$ is a zero mode. We will use the terms ‘‘Statistically Preserved Structures’’ and ‘‘zero modes’’ interchangeably.

Of course, returning to the active fields, it makes no sense to consider the decaying problem; as the active field decays, the statistics of the velocity field changes, and there is very little to say. On the other hand, we propose that it is possible to learn a great deal from considering the forced solutions, comparing the forced correlation functions of the active field with those of the passive field when advected by the same velocity field [8]. The rest of this paper is devoted to making this point clear and solid.

In Sect. II we discuss the active problem (2) in comparison with the passive problem (6). A preliminary report of the correspondence between these problems was presented in [9]. Since we are interested in points of principle rather than quantitative details, we opt to work with a shell model of the turbulent convection problem. We will argue (cf. Sect. IV) that there are excellent reasons to believe that the results found for the shell model translate verbatim to the partial differential equations. The main result of Sect. II is that the forced $2m$ th-order correlation functions of the active and passive fields are both dominated by the Statistically Preserved Structures of the decaying passive problem, i. e. the functions $Z^{(2m)}(\mathbf{r})$ of Eq. (15). The anomalous scaling exponents are the same for the passive and active *forced* correlation functions, they are universal (independent of the forcing $f(\mathbf{r}, t)$) and determined by the scaling exponents of $Z^{(2m)}(\mathbf{r})$. We present a careful discussion of the role of the statistical correlations between the forcing and the velocity field that exist in the active case, but are absent

in the passive case. In the present problem the net result of these correlations is just an amplitude factor relating the moments of the two fields. In Sect. III we turn to a shell model of magneto-hydrodynamics. On the face of it, this is a counter-example to the previous case: the active and passive fields exhibit radically different scaling exponents. The main result of this section is that nevertheless the Statistically Preserved Structures of the passive problem are shown to dominate the statistics of the active problem, but the existence of a conservation law in the latter results in an exact cancellation of the amplitude of the leading zero mode. We identify analytically the leading and subleading exponents of the passive problem, and then observe the cancellation of the leading contribution by the dynamics. The Summary section IV presents the general lesson for the statistical physics of the (nonlinear) active problem. We propose that the zero modes of the auxiliary passive fields will always have a dominant role in the statistics of active fields. The active fields will thus share the same scaling exponents as the passive fields unless there exist additional conservation laws for the active fields. In all cases the calculation of the active scaling exponents can be achieved in the context of the passive problem, which boils down to finding the zero modes of a linear operator.

II. ACTIVE AND PASSIVE SCALARS IN A MODEL OF TURBULENT CONVECTION

A. Model and numerical results

In this section we examine in detail a shell model of active and passive scalars for which the statistical object can be computed to high accuracy. We consider a model that reproduces the conservation laws and the form of coupling between the active field and the velocity field in Eqs. (1) and (2). Our model is a variant of the shell model studied in ref. [10]:

$$\frac{\partial u_n}{\partial t} = ak_n(u_{n-1}^2 - \lambda u_n u_{n+1}) + bk_n(u_n u_{n-1} - \lambda u_{n+1}^2) - \nu k_n^2 u_n + T_n , \quad (18)$$

$$\frac{\partial T_n}{\partial t} = \tilde{a}k_n(u_{n-1}T_{n-1} - \lambda u_n T_{n+1}) + \tilde{b}k_n(u_n T_{n-1} - \lambda u_{n+1} T_{n+1}) - \kappa k_n^2 T_n + f_0 \delta_{n,0} , \quad (19)$$

$$\frac{\partial C_n}{\partial t} = \tilde{a}k_n(u_{n-1}C_{n-1} - \lambda u_n C_{n+1}) + \tilde{b}k_n(u_n C_{n-1} - \lambda u_{n+1} C_{n+1}) - \kappa k_n^2 C_n + f_0 \delta_{n,0} . \quad (20)$$

In this model all the field variables are real and n stands for the index of a shell of wavevector $k_n = k_0 \lambda^n$, with $n = 0, 1, \dots, N-1$. We take $\lambda = 2$, and the parameters used in the simulation are $a = 0.01$, $\tilde{a} = \tilde{b} = b = 1$, $k_0 = 1$, $\kappa = \nu = 5 \times 10^{-4}$. The number of shells is

$N = 30$, and the forcing is white noise of zero mean on the first shell.

Without the coupling to T_n , the velocity equation has an inviscid unstable Kolmogorov fixed point, $u_n \sim k_n^{-1/3}$.

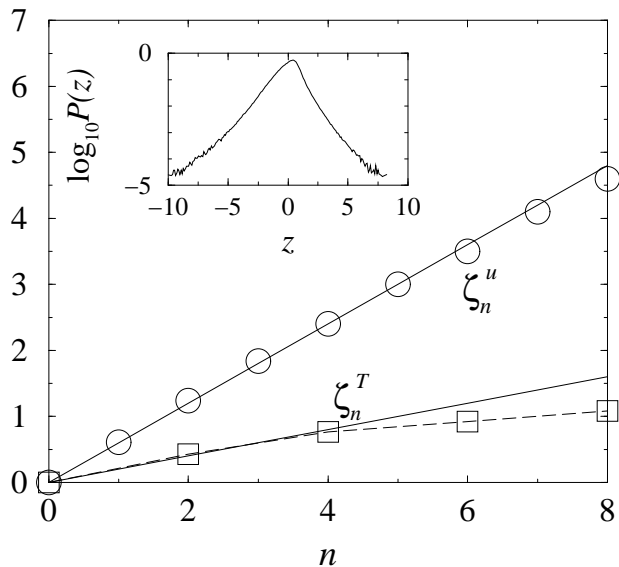


FIG. 1: The scaling exponents ζ_n^u of the velocity field (circles) and ζ_n^T of the active scalar field (squares) for even n 's. The solid lines are respectively $3n/5$ and $n/5$ for the velocity and the active scalar fields. Shown in the inset is the PDF of $z \equiv u_n / \langle u_n^2 \rangle^{1/2}$ at shell $n = 14$.

This is changed by the coupling [10], and the system of equations for T_n and u_n exhibits an inviscid unstable Bolgiano fixed point, $u_n \sim k_n^{-3/5}$, $T_n \sim k_n^{-1/5}$. The chaotic dynamics renders the statistics of the velocity field strongly non-Gaussian (cf. inset in Fig. 1). The exponents ζ_n^T for the active scalar are markedly anomalous, whereas, for the velocity, they appear closer to normal (see Fig. 1). The equation of motion for the passive field C is identical to the equation of motion of T , but it does not affect the velocity field u . This equation has a $C \rightarrow -C$ symmetry, whereas the coupled system of T and u lacks this symmetry. This difference is reflected in the statistics of the two fields.

To demonstrate this difference between the active and passive fields, we show in Fig. 2 the probability distribution functions (PDF) of $x = \phi_n / \langle \phi_n^2 \rangle^{1/2}$ where ϕ_n is T_n or C_n , for $n = 14$. One clearly sees the symmetry of the PDF of the passive scalar, in contradistinction to the asymmetry of the PDF of the active scalar. This is typical to all n in the inertial range. This is a demonstration of the discussion after Eq. (28). For the passive scalar the odd moments vanish, whereas for the active scalar they all exist. The situation is altogether different for the statistics of even moments. To demonstrate the difference we plot in Fig. 3 the (typical) PDF of \tilde{T}_n^2 and C_n^2 for $n = 9$ and 14 , where $\tilde{T}_n \equiv T_n - \langle T_n \rangle$. In plotting we realize that the passive scalar is defined up to a constant, so for the passive scalar the PDF is plotted for the rescaled variable βC_n^2 , where

$$\beta = \langle \tilde{T}_n^2 \rangle_f / \langle C_n^2 \rangle_f \approx 0.6327. \quad (21)$$

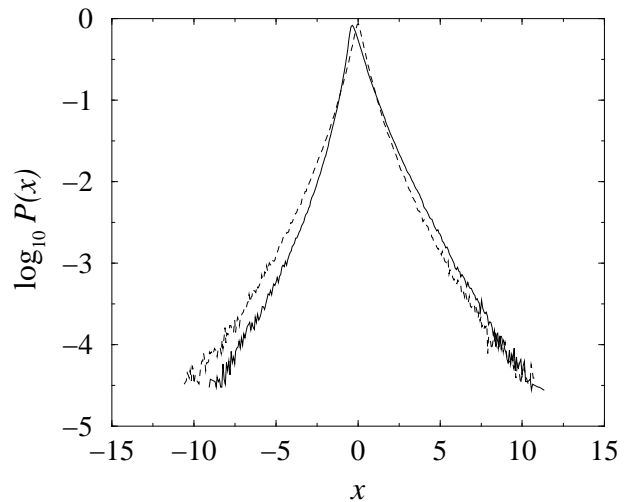


FIG. 2: The PDF's of the active (solid) and passive (dashed) scalars at shell $n = 14$. Note that the PDF of the active scalar is asymmetric.

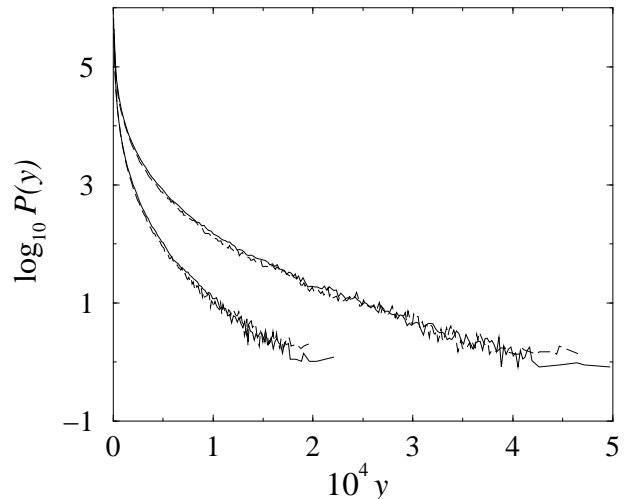


FIG. 3: The PDF's of y where $y = \tilde{T}_n^2$ (solid) or βC_n^2 (dashed) at shells $n = 9$ and 14 .

Note that there is only one numerical freedom β , constant for all n in the inertial range. An understanding of this numerical constant based on dynamical considerations is given in the next subsection.

We find very close agreement of all the PDF's in the inertial range. The identity of the PDF's of \tilde{T}_n^2 and C_n^2 translates automatically to the identity of the even-order structure functions $F^{(2m)}(k_n) \equiv \langle \tilde{\phi}_n^{2m} \rangle_f$, where $\tilde{\phi}_n = \tilde{T}_n$ or C_n (up to a constant β^m). This is demonstrated in Fig. 4. We see that the 2nd, 4th and 6th-order structure functions are barely distinguishable, with the same scaling exponents in the inertial range. Finally, we demonstrate that the identity of the statistics of the squares of the passive and active scalars transcends structure functions. Consider for example the multi-point correlation

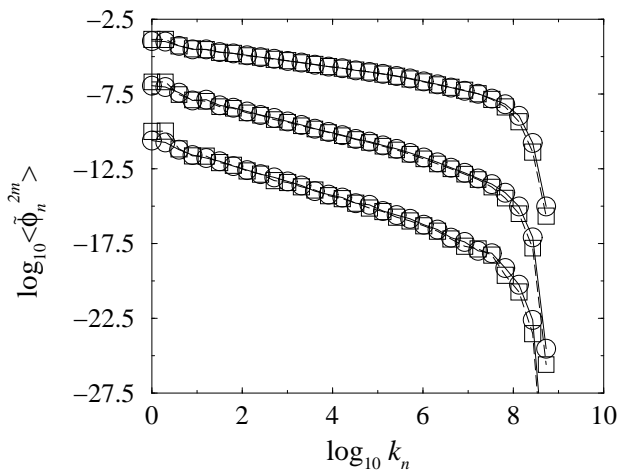


FIG. 4: The even-order structure functions $\langle \tilde{T}_n^{2m} \rangle_f$ (circles) and $\langle \beta^m C_n^{2m} \rangle_f$ (squares), with $m = 1, 2$ and 3 , from top to bottom.

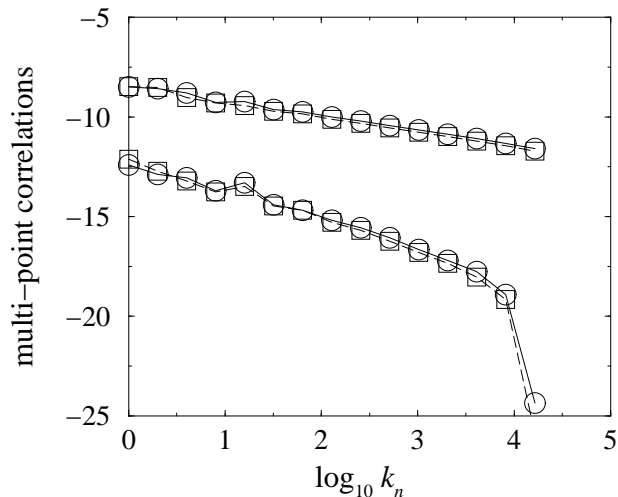


FIG. 5: Upper: $\log_{10} \langle \tilde{T}_n^2 \tilde{T}_{n+5}^2 \rangle_f$ (circles) and $\log_{10} \langle \beta^2 C_n^2 C_{n+5}^2 \rangle_f$ (squares). Lower: $\log_{10} \langle \tilde{T}_n^2 \tilde{T}_{n+5}^2 \tilde{T}_{2n}^2 \rangle_f$ (circles) and $\log_{10} \langle \beta^3 C_n^2 C_{n+5}^2 C_{2n}^2 \rangle_f$ (squares).

functions $\langle \tilde{T}_n^2 \tilde{T}_{n+5}^2 \rangle$ and $\langle \tilde{T}_n^2 \tilde{T}_{n+5}^2 \tilde{T}_{2n}^2 \rangle$. In Fig. 5 these correlation functions are compared to their passive counterparts. The conclusion is that again the multi-point correlation functions are indistinguishable once the passive ones are rescaled by β^q where q is the overall order of the correlation function.

B. Analysis of the results

To understand the results we start with the passive field, demonstrating that its forced structure functions are actually Statistically Preserved Structures. Consider then the decaying passive problem, i. e. Eq. (20) without the forcing term. The initial value problem for the time

dependent structure functions $G^{(2m)}(k_n, t) \equiv \langle C_n^{2m}(t) \rangle$ is the shell analog of Eq. (13),

$$G^{(2m)}(k_n, t) = \mathcal{P}_{n,n'}^{(2m)}(t) G^{(2m)}(k_{n'}, t=0), \quad (22)$$

which defines the $2m$ th-order propagator $\mathcal{P}_{n,n'}^{(2m)}(t)$. Here and below, repeated indices are being summed over. In Fig. 6 we show typical decay plots, for the quantity $K^{(2m)} \equiv \sum_n G^{(2m)}(k_n, t)$ for $m = 1, 2, 3$, starting from the initial conditions $G^{(2m)}(k_n, t=0) = \delta_{n,16}$.

Statistically Preserved Structures in this case represent left-eigenfunctions $Z^{(2m)}(k_n)$ of eigenvalue 1 satisfying

$$Z^{(2m)}(k_{n'}) = Z^{(2m)}(k_n) \mathcal{P}_{n,n'}^{(2m)}(t). \quad (23)$$

The statement that we want to demonstrate is that the forced structure functions $F_n^{(2m)}$ of the passive scalar scale like these eigen-modes of the decaying problem:

$$F^{(2m)}(k_n) \equiv \langle C_n^{2m} \rangle_f \sim Z^{(2m)}(k_n). \quad (24)$$

To demonstrate this we use the method of [6] and define the quantities $I^{(2m)}$,

$$I^{(2m)} = \sum_n G^{(2m)}(k_n, t) F^{(2m)}(k_n). \quad (25)$$

Using Eqs. (22) and (23) we see that if Eq. (24) is obeyed, then the quantities $I^{(2m)}$ are time independent. Indeed, in Fig. 6 we demonstrate the stationarity of these objects, thus supporting Eq. (24). The analytic explanation as to why the forced solutions agree with the Statistically Preserved Structures of the decaying problem was provided in [7]. Before turning to the active field, it is worthwhile to observe how any initial condition of the decaying passive field lands on the scaling solution that is represented by the Statistically Preserved Structure. Consider the initial value experiment that is reported in Fig. 7. Here we start, as an example, from the initial value $C_n(t=0) \propto k_n^{2/3}$. In this initial condition the order of the amplitudes is inverted with respect to the spectrum of the passive scalar. We plot, as a function of time, the trajectories of $C_n(t)$ as computed just from this initial condition, averaged over 650 realizations. We see that the trajectories land on a decaying scaling solution in which the order of the amplitudes and the ratios between them are identical to the spectrum of the zero mode of the passive field; the decay that we see, at a rate proportional to $1/t^2$, is entirely due to dissipative effects, as explained in some detail in [7].

Finally, we need to understand how the forced active scalar T falls on the Statistically Preserved Structure of the decaying passive problem, and what is the origin of the factor β in (21). To this aim we note that both equations for passive and active fields can be written as

$$\frac{\partial \phi_n}{\partial t} = \mathcal{L}_{n,n'} \phi_{n'} + f_0 \delta_{n,0}. \quad (26)$$

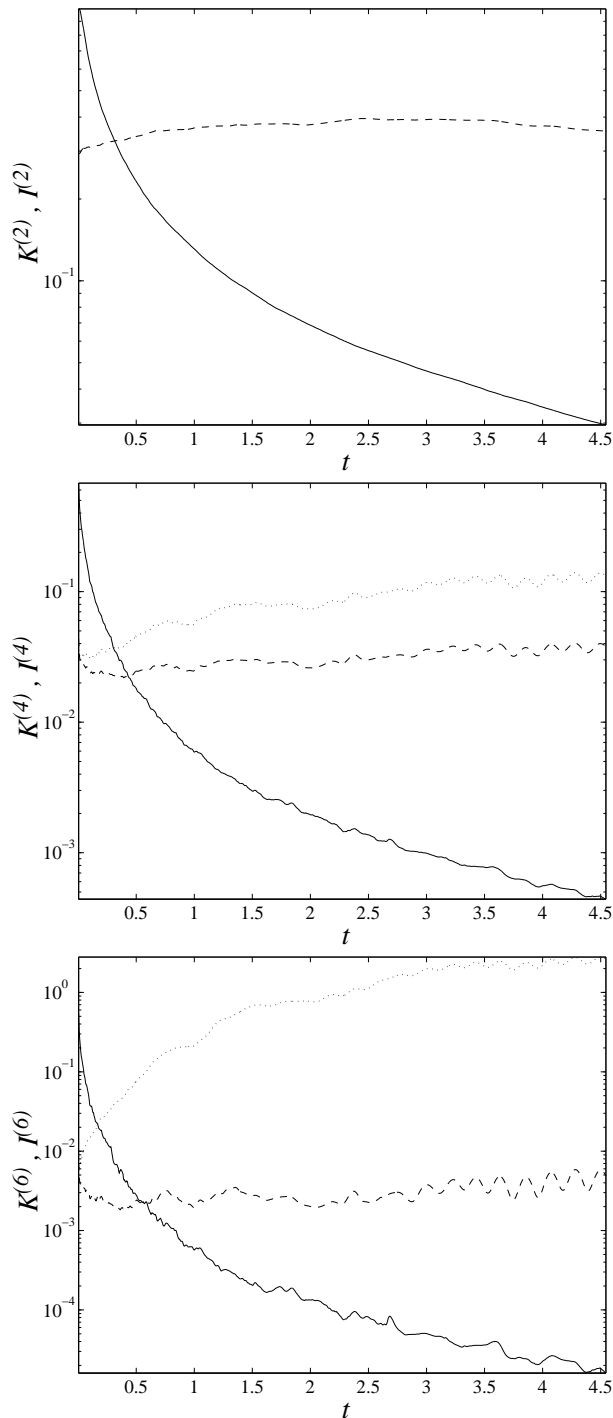


FIG. 6: The decaying objects $K^{(2m)}$ (solid lines) and the conserved objects $I^{(2m)}$ (dashed lines) as a function of time, for $m = 1, 2$ and 3 . Time is measured here in units of the largest scale eddy turn over time $\tau_0 \equiv [k_0 \sqrt{S_2(k_0)}]^{-1} \approx 22$. In panels b and c we include in dotted lines the quantity $I^{(2m)}$ in which we replaced $F^{(2m)}$ by its dimensional prediction $[F^{(2)}]^m$. We see that using the dimensional exponent does not make $I^{(2m)}$ time invariant.

This equation has a formal solution in the form

$$\phi_n(t) = R_{n,n'}(t|0)\phi_{n'}(t=0) + \int_0^t d\tau R_{n,0}(t|\tau)f_0(\tau), \quad (27)$$

where $R_{n,n'}(t|\tau)$ is the shell analog of the operator (11),

$$R_{n,n'}(t|\tau) \equiv \left\{ T^+ \int_\tau^t \exp[\mathcal{L}(s)] ds \right\}_{n,n'}. \quad (28)$$

The first difference between the active and passive fields is encountered when we take the average of this equation. For the passive case, the average can be taken by decorrelating f_0 and $R_{n,n'}$. Since the mean of the force f_0 vanishes, we get

$$\langle C_n \rangle_f = 0 \quad (29)$$

Such a decorrelation is, however, not allowed in the active case since the forcing f_0 is correlated with T , which is itself correlated with \mathbf{u} and thus with $R_{n,n'}$. Hence

$$\langle T_n \rangle_f = \langle R_{n,n'}(t|0)T_{n'}(t=0) \rangle_f + \int_0^t d\tau \langle R_{n,0}(t|\tau)f_0(\tau) \rangle_f \quad (30)$$

and T has a non-zero mean. Similarly, the passive scalar has zero odd moments and its PDF is symmetric. On the other hand, the active scalar has nonvanishing odd moments and its PDF is asymmetric.

In spite of this great difference between the active and passive scalars, there is a close affinity between the active field and the Statistically Preserved Structures of the passive field. To see this, we note that the first term on the RHS of Eq. (30) represents a decaying field. We expect that if the initial condition $T_n(t=0)$ has any component on the Statistically Preserved Structure of the passive field, it will quickly relax everything else and will land exactly on that solution. In this respect it is just the same as the initial value experiment reported in Fig. 7. In terms of the relative amplitudes of the different n shells there is nothing in the fate of the initial value term to distinguish the active and the passive fields. The second term on the RHS of Eq. (30) is more subtle. First, we note that for every value of τ we again face a decaying experiment that takes place between the times τ and t . In the language of the passive field, the integrand can be read from a decaying field with initial condition $C_n(t=\tau) = f_0(\tau)\delta_{n,0}$. Indeed, in our simulations below this is precisely how we evaluate integrals of this type. We break the interval $[0, t]$ into N sub-intervals $\{\tau_i\}_{i=1}^N$, $\tau_i = (i/N)t$, and start a decaying experiment with initial conditions $f(\tau_i)\delta_{n,0}$. Measuring $C_n(t)$ and summing up all the contributions yields an approximation to the integral. Every term in the integrand is expected to land, for most of the time $t - \tau$, on the scaling solution of the passive field, in much of the same way that the initial value term does. Thus both terms in Eq. (30) are expected to scale like the passive field, which nevertheless itself has zero amplitude due to the symmetry.

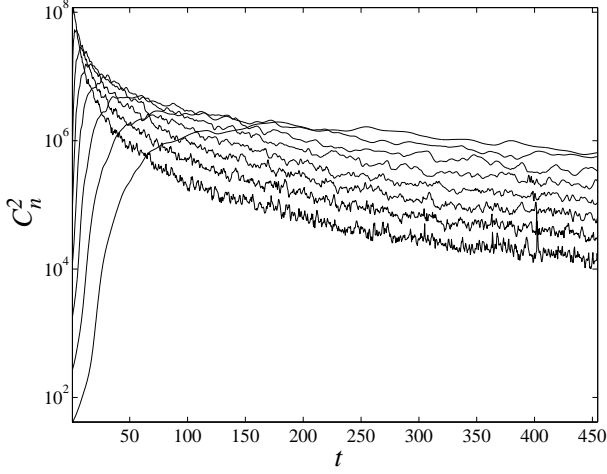


FIG. 7: An example of the fate of an initial value term as a function of time, in units of τ_0 . The initial amplitudes are inverted in order compared to the 2nd order zero modes of the passive field. Shown are shells $n = 5, 7, \dots, 19$.

The correlation effects that play a role for the active scalar will be responsible for the factor β that we discovered in the numerics. To see this we need to consider the 2nd order structure functions:

$$\begin{aligned} F^{(2)}(k_n) &= \langle [R_{n,n'}(t|0)\phi_{n'}(t=0)]^2 \rangle_f \quad (31) \\ &+ 2\langle R_{n,n'}(t|0)\phi_{n'}(t=0) \int_0^t d\tau R_{n,0}(t|\tau)f_0(\tau) \rangle_f \\ &+ \int_0^t d\tau' d\tau'' \langle R_{n,0}(t|\tau')R_{n,0}(t|\tau'')f_0(\tau')f_0(\tau'') \rangle_f . \end{aligned}$$

For sufficiently long time the first two terms, denoted below as \mathcal{I}_1 and \mathcal{I}_2 respectively, do not contribute to the structure functions, and any difference between the active and passive fields must be ascribed to the last term. The last term, denoted here as \mathcal{I}_3 , has a “diagonal” contribution, which is obtained for $\tau' = \tau''$ and an “off-diagonal” contribution, which is the rest of the integral for which $\tau' \neq \tau''$. For the passive field, $R_{n,n'}$ and f_0 decouple and only the diagonal part exists. For the active field there is no decoupling. Denoting this term $\mathcal{I}_{3,d}$, it reads respectively

$$\mathcal{I}_{3,d} = \int ds \langle R_{n,0}(t|s)R_{n,0}(t|s) \rangle_f f_0^2 \quad (\text{passive}) , \quad (32)$$

$$\mathcal{I}_{3,d} = \int_0^t ds \langle R_{n,0}(t|s)R_{n,0}(t|s)f_0(s)f_0(s) \rangle_f \quad (\text{active}) \quad (33)$$

In Fig. 8 we compare the integrands of these two expressions, measured directly in our simulation as explained above. We can see that there is not much difference between them; the diagonal term cannot be blamed for the factor β . On the other hand, in Fig. 9 we show the full integral \mathcal{I}_3 and compare it with its diagonal term. We see that in the passive case the diagonal part is everything, whereas in the active case there is a

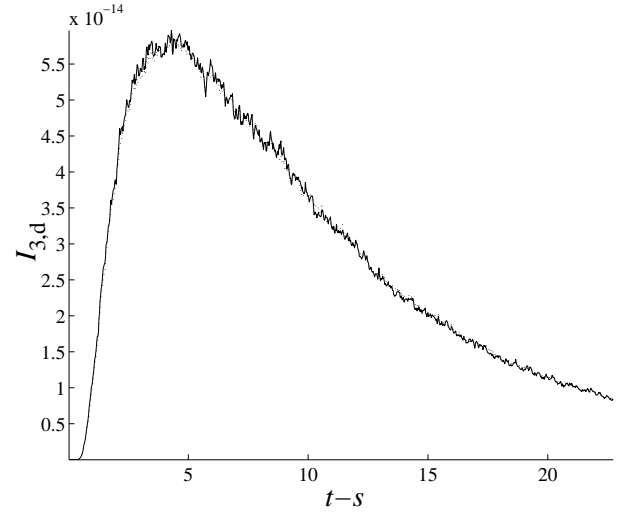


FIG. 8: Comparison of the integrands in Eqs (32) (the passive case) and (33) (the active case) for $n = 10$. The plots are indistinguishable.

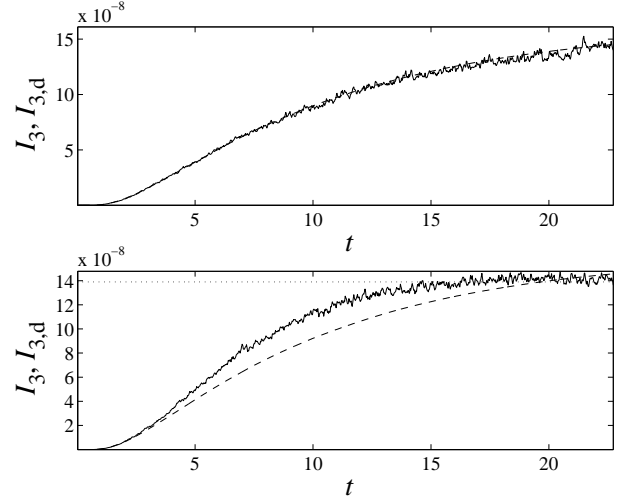


FIG. 9: The integral \mathcal{I}_3 in comparison to the diagonal part $\mathcal{I}_{3,d}$ for $n = 10$. Upper panel: the passive field. The integral agrees with the diagonal part at all times. Lower panel: the active field. The deviations are due to the non-vanishing contribution of the off-diagonal integral, which is also displayed in the next figure. The dashed line in both panels represents the stationary value of the corresponding second order structure function.

difference. Lastly, we show that this difference is precisely the source of the factor β . In Fig. 10 we show $\langle [\phi_n(t) - R_{n,n'}(t|0)\phi_{n'}(t=0)]^2 \rangle - \mathcal{I}_{3,d}$ for the passive and the active fields. The former fluctuates all the time around zero. The latter is positive initially, and then becomes negative. For later times it saturates at a negative value that is precisely responsible for the factor β .

In summary, we find that the even correlation functions of the active and passive scalars share the same scaling

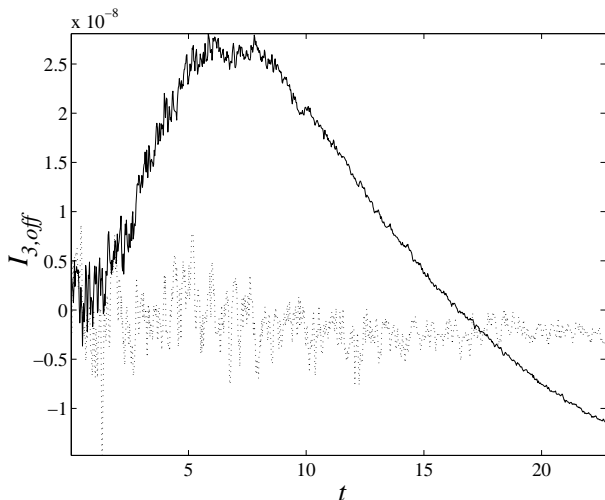


FIG. 10: The off-diagonal integral for $n = 10$, computed as $\langle [\phi_n(t) - R_{n,n'}(t|0)\phi_{n'}(t=0)]^2 \rangle - \mathcal{I}_{3,d}$ for the passive and active fields respectively. For the passive field (dotted line) it fluctuates around zero, while for the active field it begins positive, and then turns negative. For longer times it saturates at a constant negative value, giving rise to the factor β .

exponents simply because the zero modes of the decaying passive problem dominate the statistics of both fields. It is thus possible to understand the anomalous statistics

of the active field in the same way as that of the passive field. We believe that this is a significant result that should be put to further experimental and numerical tests in the PDE version of the problem. We will return to this point in the discussion.

III. ACTIVE AND PASSIVE FIELDS IN A MODEL OF MAGNETOHYDRODYNAMICS

A. Model and Numerical Results

In this section we examine a shell model that reproduces the type of coupling and the conservation laws of Eqs. (3). We need to be careful about the dynamo effect which we want to avoid in order to have stationary statistics. We thus construct the model to mimic 2-dimensional MHD, in which there is an inverse cascade of energy. Accordingly we need to have large scale damping terms in the velocity equation, and a force at intermediate scales. In all our simulations below we force both the velocity and the active fields on shells 10 and 11 (denoted by n_f), using white noise of zero mean. We run the model with 35 shells. The equations are an adaptation of the MHD shell model of [11] to the Sabra shell model [12]. All field variables are complex numbers:

$$\begin{aligned} \frac{du_n}{dt} = & ik_n [a\lambda(u_{n+1}^*u_{n+2} - b_{n+1}^*b_{n+2}) + b(u_{n-1}^*u_{n+1} - b_{n-1}^*b_{n+1}) - c\lambda^{-1}(u_{n-2}u_{n-1} - b_{n-2}b_{n-1})] \\ & + f'_n \delta_{n,n_f} + \nu k_n^2 u_n + \tilde{\nu} k_n^{-4} u_n, \end{aligned} \quad (34)$$

$$\begin{aligned} \frac{db_n}{dt} = & ik_n [\tilde{a}\lambda(u_{n+1}^*b_{n+2} - b_{n+1}^*u_{n+2}) + \tilde{b}(u_{n-1}^*b_{n+1} - b_{n-1}^*u_{n+1}) - \tilde{c}\lambda^{-1}(u_{n-2}b_{n-1} - b_{n-2}u_{n-1})] \\ & + f_n \delta_{n,n_f} + \kappa k_n^2 b_n + \tilde{\kappa} k_n^{-4} b_n. \end{aligned} \quad (35)$$

The coefficients a , b , c , \tilde{a} , \tilde{b} and \tilde{c} can be parametrized as follows :

$$\begin{aligned} a = 1, \quad b = -\delta, \quad c = -(1-\delta), \\ \tilde{a} = 1 - \delta - \delta_m, \quad \tilde{b} = \delta_m, \quad \tilde{c} = 1 - \delta_m. \end{aligned} \quad (36)$$

This choice ensures the conservation of the total energy and “cross helicity” in the inviscid limit $\nu = \tilde{\nu} = \kappa = \tilde{\kappa} = f = f' = 0$,

$$E = \frac{1}{2} \sum_n (|u_n|^2 + |b_n|^2), \quad (37)$$

$$K = \sum_n \Re(u_n^* b_n). \quad (38)$$

To mimic the magnetic helicity, we can write down a generalized quantity

$$H = \frac{1}{2} \sum_n \text{sign}(\delta - 1)^n \frac{|b_n|^2}{k_n^\alpha}, \quad (39)$$

with $\alpha > 0$ a fixed parameter. We demand conservation of this generalized “magnetic helicity”, together with absence of dynamo effect. This implies

$$\delta > 1 \rightarrow \begin{cases} \delta = 1 + \lambda^{-\alpha}, \\ \delta_m = -1/(\lambda^\alpha - 1), \end{cases} \quad (40)$$

On the other hand, when $\delta < 1$ one can have dynamo, and therefore no stationary statistics.

In addition to the conservation laws the equations of motion remain invariant to the phase transformations

$u_n \rightarrow u_n \exp(i\phi_n)$ and $b_n \rightarrow b_n \exp(i\psi_n)$. The conditions are

$$\phi_n + \phi_{n+1} - \phi_{n+2} = 0, \quad (41)$$

$$\phi_n + \psi_{n+1} - \psi_{n+2} = 0, \quad (42)$$

$$\psi_n + \phi_{n+1} - \psi_{n+2} = 0, \quad (43)$$

$$\psi_n + \psi_{n+1} - \phi_{n+2} = 0. \quad (44)$$

This implies $\psi_n = \phi_n \forall n$.

The passive field is denoted by q_n , whose evolution is given by an equation similar to Eq. (35), i. e.

$$\begin{aligned} \frac{dq_n}{dt} = & ik_n[\tilde{a}\lambda(u_{n+1}^*q_{n+2} - q_{n+1}^*u_{n+2}) + \tilde{b}(u_{n-1}^*q_{n+1} - q_{n-1}^*u_{n+1}) - \tilde{c}\lambda^{-1}(u_{n-2}q_{n-1} - q_{n-2}u_{n-1})] \\ & + \kappa k_n^2 q_n + f_n \delta_{n,n_f}. \end{aligned} \quad (45)$$

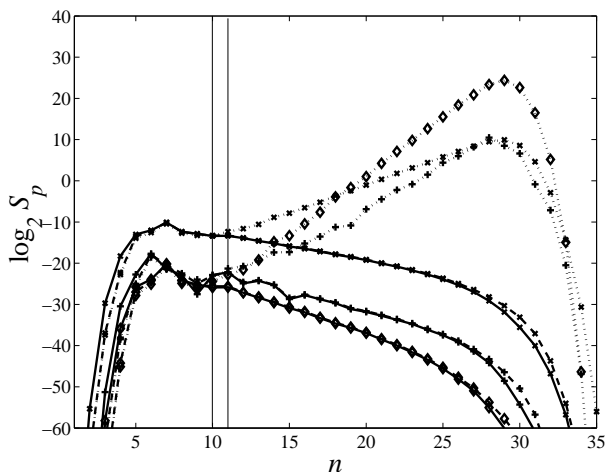


FIG. 11: Structure functions of order 2 (\times), 3 ($+$) and 4 (\diamond) for the passive field (dotted line), active field (dashed line) and velocity field (solid line). The two vertical lines denote the forcing shells. Note that the scaling exponents of the active field and the velocity field coincide. The parameters are $N = 35$, $\alpha = 2$, $k_0 = 0.0625$, $\nu = 10^{-12}$, $\tilde{\nu} = 10^{-3}$. The forcing is white noise on shells 10,11.

The fields q_n and b_n are advected by the same velocity field, however b_n is active, while q_n is passive. The inviscid passive equation has only one conserved variable, i. e. Eq. (39) with q_n replacing b_n . It also satisfies the same phase relations as the active field. We want to know whether the scaling properties of b_n are determined once again by the Statistically Preserved Structures of the decaying problem of the passive field q_n .

In Fig. 11 we show the spectra of the passive and active fields respectively, obtained from a direct numerical simulation with the parameters as detailed in the figure legend. This appears like a striking counter-example to the results of the previous section: the two fields have totally different scaling behaviors. The active field has “standard” scaling exponents η_p , defined by $\langle |b_n|^p \rangle \sim k_n^{-\eta_p}$, that coincide with those of the velocity field, defined by

$\langle |u_n|^p \rangle \sim k_n^{-\zeta_p}$, and the spectrum decays like a power law in the “inertial range” which is between the forcing and the dissipative scales. We estimate from the numerics $\eta_2 = \zeta_2 \approx .67$, $\eta_3 = \zeta_3 \approx 1.0$ and $\eta_4 = \zeta_4 \approx 1.33$, in close correspondence with the Kolmogorov dimensional predictions. The passive field has exponents, defined similarly by $\langle |q_n|^p \rangle \sim k_n^{-\beta_p}$, that are with a different sign! Its spectrum is an increasing function of k_n in the inertial range. We measure $\beta_2 \approx -1.33$, $\beta_3 \approx -2$ and $\beta_4 \approx -2.67$. If we assume that the passive field lands on the Statistically Preserved Structures of the passive decaying problem, then it appears that the active field does not do so.

In the rest of this section we will show that this is actually not a counterexample to the proposition that the active field lands on Statistically Preserved Structures of the decaying passive field. It does. What happens here is that, due to the conservation law Eq. (38), the amplitude of the leading Statistically Preserved Structure with the negative scaling exponent is exactly zero. The active field then lands on a sub-leading zero mode, which has standard, positive scaling exponent (the positive sign refers to \mathbf{r} -space representation, as in Eq. (5)).

B. Analysis of the results

To gain insight into this interesting situation we note that the analog of Eq. (28) describes the dynamics of our active field b_n :

$$b_n(t) = R_{n,n'}(t|0)b_{n'}(t=0) + \int_0^t d\tau R_{n,n_f}(t|\tau)f_{n_f}(\tau), \quad (46)$$

with an obvious re-definition of the present operator $R_{n,n'}$. It is very revealing to examine the time dependence of the two terms on the RHS of this equation. We measure time in units of the eddy turn over time of the forcing shell 10. This is defined as $\tau_{10} \equiv [k_{10}\sqrt{\langle |u_{10}|^2 \rangle}]^{-1} \approx 3.35$. We will examine a forced system which began running at $t = -\infty$, denoting a generic time as $t = 0$. In Fig. 12 panel a we show the time-dependence of the first term for 6 values of n in the in-

ertial interval. We see that the initial conditions represent, as expected, a 'standard' spectrum in which the amplitude b_n decreases as a function of n . As time proceeds, the decaying term cannot recognize its being 'active' from being 'passive', and it switches rapidly to the Statistically Preserved Structure of the decaying passive field, characterized by a negative exponent. If it were not for the second term on the RHS of Eq. (46), then b_n would have landed on the same solution as q_n . What about the second term? In panel b of Fig. 12 we show the n dependence of the term at time $t = 3 \times 10^{-4}$. We see that also this term agrees, in its n dependence, with the negative exponent of the passive field. Yet, the LHS $b_n(t)$ fluctuates around *decreasing* amplitudes as n increases, meaning that the leading (negative) exponent exactly cancels between the two terms on the RHS of Eq. (46). We demonstrate this cancellation in Fig. 13. There we plot the real parts of the initial value term and the integral term at time $t = 0.3$. We see that the two terms cancel each other. The imaginary parts exhibit the same behavior.

Next we need to understand this cancellation from the analysis of the equations of motion. With this analysis we will also show that the solution on which $b_n(t)$ is landing is also a Statistically Preserved Structure of the decaying passive field, albeit with a sub-leading scaling exponent.

C. Statistically Preserved Structures of the passive field

In the next subsection we will show that the velocity field attains a scaling solution with $\zeta_3 = 1$:

$$S_3(k_n) \equiv \Im \langle u_{n-1} u_n u_{n+1}^* \rangle_f \sim k_n^{-1}. \quad (47)$$

where \Im denotes the imaginary part. In this section we will assume this, and examine what are the scaling solutions that agree with the existence of a 2nd order Statistically Preserved Structure for the passive field. We are not going to compute the anomalous scaling exponent exactly, but rather obtain their dimensional estimates. Since we are after a radically different apparent behavior, small numerical corrections are not our main concern. With this caveat in mind, we can calculate the exponent β_3 characterizing the third order structure function

$$P_3(k_n) \equiv \Im \langle q_{n-1} q_n q_{n+1}^* \rangle \sim k_n^{-\beta_3}. \quad (48)$$

The condition for the existence of the 2nd order Statistically Preserved Structure is

$$\frac{d}{dt} \langle |q_n|^2 \rangle = 0, \quad \forall n, \quad (49)$$

in the inviscid limit. Using Eq. (45) this condition generates a number of third order quantities that need to be analyzed first. Denote therefore

$$\begin{aligned} Q_{3,1}(k_n) &\equiv \Im \langle u_{n-1} q_n q_{n+1}^* \rangle, \\ Q_{3,2}(k_n) &\equiv \Im \langle q_{n-1} u_n q_{n+1}^* \rangle, \\ Q_{3,3}(k_n) &\equiv \Im \langle q_{n-1} q_n u_{n+1}^* \rangle. \end{aligned} \quad (50)$$

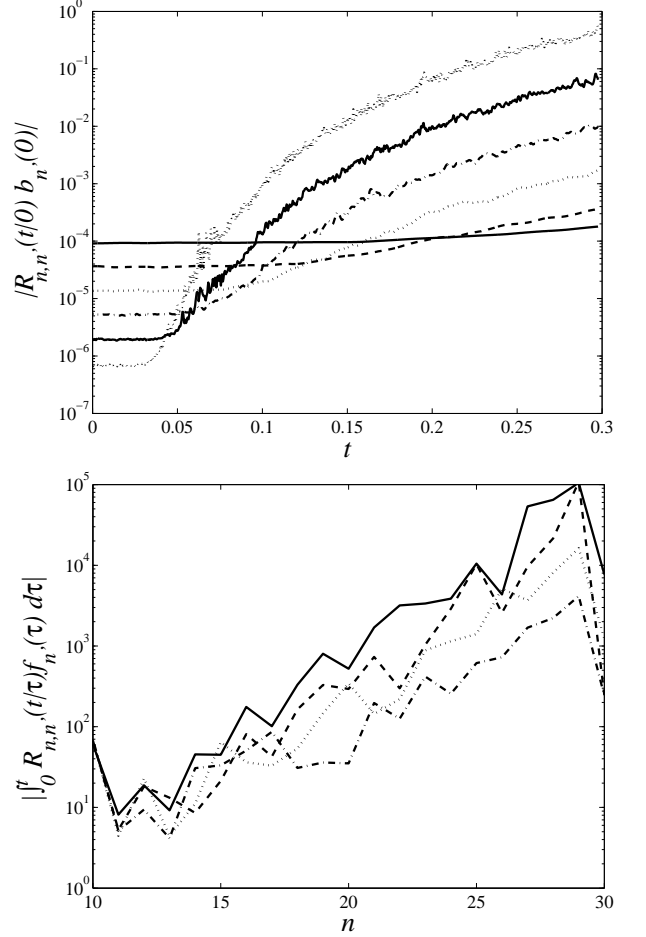


FIG. 12: Panel a: The fate of the modulus of the initial value term, averaged over 2,000 realizations. Shown are shells 15, 17, 19, 21, 23 and 25 (top to bottom from the left-most side). At time $t = 0$ their relative amplitudes agree with the scaling exponent of the *active* field. As time progresses the decaying field switches to the relative amplitudes which agree with the scaling exponent of the *passive* field. Panel b: The modulus of four realizations of the integral as a function of n , for time $t = 3 \times 10^{-4}$ (in unit of τ_{10}). Note that both terms of the RHS of Eq. (46) exhibit the same *leading* scaling behavior. This is canceled exactly as is demonstrated in Fig. 13

In order to construct scaling solutions for these objects, Dimensional consideration imply that the fields involved in the averages above have scalings $u_n \propto \lambda^{-n/3}$ and $q_n \propto \lambda^{-\beta_3 n/3}$. We infer the expressions

$$\begin{aligned} Q_{3,1}(k_n) &= |q_0|^2 |u_0| k_n^{-(2\beta_3+1)/3} \lambda^{-(\beta_3-1)/3}, \\ Q_{3,2}(k_n) &= |q_0|^2 |u_0| k_n^{-(2\beta_3+1)/3}, \\ Q_{3,3}(k_n) &= |q_0|^2 |u_0| k_n^{-(2\beta_3+1)n/3} \lambda^{(\beta_3-1)/3}. \end{aligned} \quad (51)$$

We can thus rewrite

$$Q_{3,1}(k_n) \equiv \lambda^{-(\beta_3-1)/3} \tilde{Q}_3(k_n), \quad (52)$$

$$Q_{3,2}(k_n) \equiv \tilde{Q}_3(k_n), \quad (53)$$

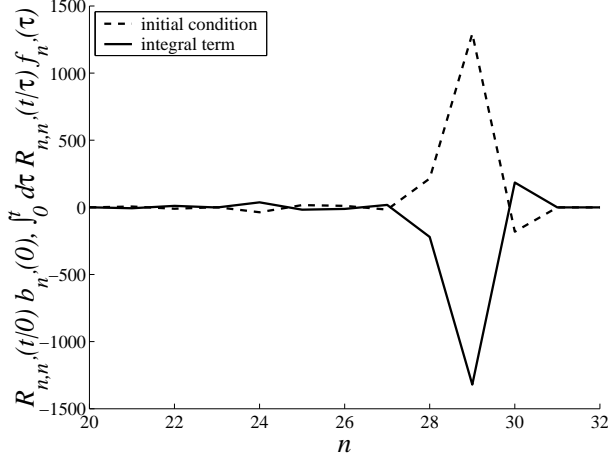


FIG. 13: the real part of the initial value term (dashed line) and integral term (solid line) as a function of k_n . This is a demonstration of the cancellation of the leading order term in favor of the subleading one. The imaginary parts behave in the same way.

$$Q_{3,3}(k_n) \equiv \lambda^{(\beta_3-1)/3} \tilde{Q}_3(k_n), \quad (54)$$

where $\tilde{Q}_3(k_n)$ scales like

$$\tilde{Q}_3(k_n) \equiv \lambda^{-(2\beta_3+1)n/3}. \quad (55)$$

having these definitions in mind we derive, by demanding Eq. (49) and substituting the scaling form of \tilde{Q}_3 Eq. (55), the equation

$$\tilde{a}\lambda^{-(2\beta_3-2)/3}(1 - \lambda^{(\beta_3-1)/3}) + \tilde{b}(\lambda^{-(\beta_3-1)/3} - \lambda^{(\beta_3-1)/3}) + \tilde{c}\lambda^{(2\beta_3-2)/3}(\lambda^{-(\beta_3-1)/3} - 1) = 0. \quad (56)$$

This is a fourth order polynomial in $\lambda^{(\beta_3-1)/3}$. The four roots are

$$\lambda^{(\beta_3-1)/3} = \begin{cases} 1, \\ \lambda^{-\alpha}, \\ \pm \lambda^{-\alpha/2}. \end{cases} \quad (57)$$

Here three of the roots correspond to a priori physical solutions:

$$\beta_3 = \begin{cases} 1, \\ 1 - 3\alpha/2, \\ 1 - 3\alpha. \end{cases} \quad (58)$$

In our simulations with $\alpha = 2$ these results are $\beta_3 = 1, -2$ and -5 respectively. This is in agreement with spectral

exponents β_2 of the order of (neglecting anomalies) $\beta_2 = 2/3, -4/3, -10/3$. To know which of these is physical, we need to consider the fluxes supported by these solutions.

The only flux that is relevant for the passive field is the magnetic helicity. For the case considered here with $\delta > 1$ it can be conveniently computed at the shell M by evaluating

$$\Phi_M^H \equiv -\frac{1}{2} \frac{d}{dt} \sum_{n=0}^M \left\langle \frac{|q_n|^2}{k_n^\alpha} \right\rangle. \quad (59)$$

Using the equations of motion to evaluate this object we find

$$\begin{aligned} \Phi_M^H = & -\delta_m \left[k_{M+1}^{1-\alpha} (\Im \langle q_M u_{M+1} q_{M+2}^* \rangle - \Im \langle q_M q_{M+1} u_{M+2}^* \rangle) \right. \\ & \left. + k_M^{1-\alpha} (\Im \langle q_{M-1} u_M q_{M+1}^* \rangle + \Im \langle u_{M-1} q_M q_{M+1}^* \rangle) \right]. \end{aligned} \quad (60)$$

We can evaluate now the magnetic helicity flux for the three scaling solutions (58). We find

$$\Phi_M^H \propto \begin{cases} \lambda^{-\alpha M}, \\ 1, \\ \lambda^{\alpha M}. \end{cases} \quad (61)$$

We conclude that the third solution is unphysical, since it supports a flux that diverges with M . The first two solutions are allowed. With $\beta_3 = -2$ we get a constant flux;

this is the leading scaling solution, and is indeed realized in the simulations. The solution $\beta_3 = 1$ is subleading, it is associated with a decaying flux, and is asymptotically allowed. It is not observed in the passive field simulations simply because it is subleading.

Our main point will be that the *active* field will in its turn land on the subleading Statistically Preserved Structure because the additional conservation laws exclude the leading one. We demonstrate this phenomenon in the next subsection.

D. Why does the active field fall on a subleading zero mode?

If we accept the general philosophy that active fields exhibit scaling behaviors that are determined by the zero modes of the auxiliary passive fields, then we should explain here why in the present case the active field avoids the *leading* zero mode, and appears to land on the sub-

leading one. The answer is hidden of course in the conservation laws, as we expose now.

We first repeat the analysis performed in the previous section to find the consequence of the equation

$$\frac{d}{dt} \langle |b_n|^2 \rangle = 0, \quad (62)$$

or, equivalently,

$$\frac{d}{dt} \langle |u_n|^2 \rangle = 0. \quad (63)$$

Using now the definitions

$$\begin{aligned} B_3(k_n) &= \Im \langle b_{n-1} b_n b_{n+1}^* \rangle \sim k_n^{-\eta_3} \\ Q_3(k_n) &\equiv k_n^{-(2\eta_3 + \zeta_3)/3}, \end{aligned} \quad (64)$$

we obtain an equation that is analogous to Eq. (56),

$$\tilde{a} \lambda^{1-(2\eta_3 + \zeta_3)/3} (1 - \lambda^{(\eta_3 - \zeta_3)/3}) + \tilde{b} (\lambda^{-(\eta_3 - \zeta_3)/3} - \lambda^{(\eta_3 - \zeta_3)/3}) + \tilde{c} \lambda^{-1+(2\eta_3 + \zeta_3)/3} (\lambda^{-(\eta_3 - \zeta_3)/3} - 1) = 0. \quad (65)$$

This is a fourth degree polynomial for $\lambda^{\eta_3/3}$ if ζ_3 is known. Obviously, if we simply substituted here $\zeta_3 = 1$ we would get the same predictions for η_3 as obtained for β_3 in Eq. (58). However, we have in this case an important additional constraint that is absent in the case of the passive field, which can be inferred from the additional conservation equation

$$\frac{d}{dt} \Re \langle u_n^* b_n \rangle = 0 \quad (66)$$

Repeating the analysis as above, and introducing a new object $A_3(k_n) \equiv k_n^{-(\eta_3 + 2\zeta_3)}$ yields the two equations

$$\begin{aligned} a \lambda B_3(k_{n+1}) + b B_3(k_n) + c \lambda^{-1} B_3(k_{n-1}) &= 0, \quad (67) \\ a \lambda^{1-(\eta_3 - \zeta_3)/3} A_3(k_{n+1}) + b A_3(k_n) \\ + c \lambda^{-1+(\eta_3 - \zeta_3)/3} A_3(k_{n-1}) &= 0, \quad (68) \end{aligned}$$

Solving this system together with Eq. (65) yields the scaling exponents

$$\zeta_3, \eta_3 = \begin{cases} 1 \\ 1 + \log_\lambda(a/c) \end{cases}. \quad (69)$$

It is easy to check that, among the four possible combinations of this equation, the only solution allowed by Eq. (65) is

$$\zeta_3 = \eta_3 = 1. \quad (70)$$

We thus conclude that as far as the active field is considered, the additional conservation law rules out the leading zero mode of the passive problem, leaving us only with the subleading mode which is observed in the simulations.

IV. SUMMARY AND CONCLUSIONS

In this paper we considered the correspondence between the statistics of active fields that are advected by a turbulent velocity field, and the statistics of an auxiliary passive field that is advected by the same velocity, but does not affect it. The two examples were akin to turbulent convection and to magneto-hydrodynamics respectively. In the first example the conserved variables for the equations of the passive and active fields are the same. For the second example the active problem exhibits additional conservation laws. This was shown to be very significant in determining the respective statistical physics of the two problems.

The two examples appear very different in superficial examination. In the first example the even-order statistics of the passive and active fields turned out to be the same up to a single multiplicative factor β , common to all orders. The forced structure functions of the active field scale with exactly the same exponents as the passive field, which in turn are dominated by the leading zero modes of the decaying problem. We analyzed in detail the source of the multiplicative factor β and showed that it stems from the additional correlation effects between the forcing and the velocity field that are absent in the passive case. Nevertheless these correlation effects do not cause a change in the scaling exponents. The general lesson that we would propose on the basis of this example is that whenever there exist a problem in which the equation of motion of the active field does not sat-

isfy additional conservation laws compared to the passive case, the former field will exhibit structure functions that are dominated by the leading zero modes of the latter. This point is also pertinent to the second example. Here the active equations possess additional conservation laws, and indeed the active and passive fields exhibit different scaling exponents. Nevertheless we argued that the structure functions of the active field are still dominated by the zero modes of the passive problem, but not the leading ones. The additional conservation laws results in exact cancellations in the contributions of the leading zero modes, and the active problem lands on the next allowed sub-leading zero mode of the passive problem.

As a generalization, consider then a sufficiently turbulent velocity field which advects an active field, scalar or vector, which in its turn is forced by a force having a compact support in \mathbf{k} space. An auxiliary passive field which is advected by the same velocity field can be employed to find the zero modes of the operator involved in the passive decay problem. On the basis of the intuition gained with the examples presented above, we offer the following tentative conjecture: the forced structure function of the active field will exhibit scaling exponents that are the scaling exponents of the aforementioned zero modes. Whenever the conservation laws of the active and passive problems coincide, these will be the exponents of the leading zero modes. When the active problem has additional conservation laws, these will be the next-leading zero modes, as allowed by the conservation laws.

Finally, we need to consider the relation of our shell

models to the physical problems and the PDE's that motivate these models. It is important to test the conjecture stated here in that context. In light of the above discussion we expect that much of what has been found here will translate literally to the continuous problems. After all, the crucial aspects are the linearity of the advection equation, and the existence of conservation laws. These are unchanged in the continuous problems. Of course, one can expect many more numerical difficulties, especially due to the role of angles in the multi-point correlation functions. Nevertheless, the idea that the understanding of the anomalous scaling exponent of active fields boils down to the analysis of eigenfunctions of a linear operator is expected to hold verbatim.

Acknowledgments

This work has been supported in part by the Research Grants Council of Hong Kong SAR, China (CUHK 4119/98P and CUHK 4286/00P), the European Commission under a TMR grant, by the Minerva Foundation, Munich, Germany, the German Israeli Foundation, and the Naftali and Anna Backenroth-Bronicki Fund for Research in Chaos and Complexity. TG thanks the Israeli Council for Higher Education and the Feinberg postdoctoral Fellowships program at the WIS for financial support.

-
- [1] A. S. Monin and A. M. Yaglom, *Statistical Fluid Mechanics*, (MIT, Cambridge 1971).
 - [2] Ya. B. Zeldovich, A. A. Ruzmaikin and D. D. Sokoloff, *Magnetic Fields in Astrophysics* Gordon and Breach Publ. (1983).
 - [3] D. Biskamp, *Nonlinear Magnetohydrodynamics* (Cambridge, Cambridge UK, 1993)
 - [4] G. Falkovich, K. Gawedzki and M. Vergassola, *Rev. Mod. Phys.* **73**, 2001, and references therein.
 - [5] A. Celani and M. Vergassola, *Phys. Rev. Lett.* **86**, 424 (2001).
 - [6] I. Arad, L. Biferale, A. Celani, I. Procaccia and M. Vergassola, *Phys. Rev. Lett.* **87**, 164502 (2001).
 - [7] Y. Cohen, T. Gilbert and I. Procaccia, *Phys. Rev. E*, **65**, 026314 (2002).
 - [8] A. Celani, T. Matsumoto, A. Mazzino and M. Vergassola, *Phys. Rev. Lett.* **88**, 054503 (2002).
 - [9] E. S. C Ching, Y. Cohen, T. Gilbert and I. Procaccia “Statistically Preserved Structures and Anomalous Scaling in Turbulent Active Scalar Advection”, submitted to *Europhys. Lett.*, arXiv:nlin/CD/0111030.
 - [10] A. Brandenburg, *Phys. Rev. Lett.*, **69**, 605 (1992).
 - [11] P. Giuliani and V. Carbone, *Europhys. Lett.* **43**, 527 (1998).
 - [12] V. S. L'vov, E. Podivilov, A. Pomyalov, I. Procaccia and D. Vandembroucq, *Phys. Rev. E***58**, 1811 (1998).